

## Modified Pharmacokinetic/Pharmacodynamic model for electrically activated silver-titanium implant system

Zhuo Tan<sup>1,2a</sup>, Paul E. Orndorff<sup>3b</sup> and Rohan A. Shirwaiker<sup>\*1,2,4</sup>

<sup>1</sup>*Edward P. Fitts Department of Industrial and Systems Engineering, North Carolina State University, Raleigh, NC 27695, USA*

<sup>2</sup>*Medical Implants and Tissue Engineering (MITE) Lab, North Carolina State University, Raleigh, NC 27695, USA*

<sup>3</sup>*Department of Population Health and Pathobiology, North Carolina State University, Raleigh, NC 27607, USA*

<sup>4</sup>*UNC-NCSU Joint Department of Biomedical Engineering, Raleigh, NC 27695, USA*

*(Received May 9, 2015, Revised June 16, 2015, Accepted July 11, 2015)*

**Abstract.** Silver-based systems activated by low intensity direct current continue to be investigated as an alternative antimicrobial for infection prophylaxis and treatment. However there has been limited research on the quantitative characterization of the antimicrobial efficacy of such systems. The objective of this study was to develop a semi-mechanistic pharmacokinetic/pharmacodynamic (PK/PD) model providing the quantitative relationship between the critical system parameters and the degree of antimicrobial efficacy. First, time-kill curves were experimentally established for a strain of *Staphylococcus aureus* in a nutrient-rich fluid environment over 48 hours. Based on these curves, a modified PK/PD model was developed with two components: a growing silver-susceptible bacterial population and a depreciating bactericidal process. The test of goodness-of-fit showed that the model was robust and had good predictability ( $R^2 > 0.7$ ). The model demonstrated that the current intensity was positively correlated to the initial killing rate and the bactericidal fatigue rate of the system while the anode surface area was negatively correlated to the fatigue rate. The model also allowed the determination of the effective range of these two parameters within which the system has significant antimicrobial efficacy. In conclusion, the modified PK/PD model successfully described bacterial growth and killing kinetics when the bacteria were exposed to the electrically activated silver-titanium implant system. This modeling approach as well as the model itself can also potentially contribute to the development of optimal design strategies for other similar antimicrobial systems.

**Keywords:** Pharmacokinetic/Pharmacodynamic model; antimicrobial efficacy; orthopaedic implants; silver oligodynamic iontophoresis; low intensity direct current; parameter characterization; time-kill curves

### 1. Introduction

Orthopaedic implants are widely used in the treatment of musculoskeletal trauma and diseases

---

\*Corresponding author, Ph.D., E-mail: rashirwaiker@ncsu.edu

<sup>a</sup>Ph.D., E-mail: ztan@ncsu.edu

<sup>b</sup>Ph.D., E-mail: paul\_orndorff@ncsu.edu

to repair or replace the function of affected joints, fractured bone segments and impaired limbs. The global market for orthopedic devices is estimated to increase from \$21.1 billion in 2007 to \$46.5 billion in 2017 (Harris Williams & Co., 2011). A major complication associated with orthopaedic implants is the risk of infection; it is one of the leading causes of joint arthroplasty failure. Across the board, an average of 5% of all primary internal fixation devices become infected (Virk and Osmon 2001). Such infection can have adverse socio-economic consequences. For example, revision total knee arthroplasty caused by infection has an average cost of \$109,805, which is approximately 5.23 times more compared to a non-infected revision (Berbari *et al.* 1998). They also impact the psychological morbidity of patients, impairing joint function and quality of life, and sometimes requiring arthrodesis, permanent removal of the prosthesis, or even amputation (Wiedel 2002). The increasing demand for orthopaedic implants, the potential risk and consequences of implant-associated infection, and concerns over excessive antibiotic use which can lead to intractable bacterial resistance have motivated the development of new alternative antimicrobial approaches.

Recently, silver-based systems activated by low intensity direct current (LIDC) have been investigated because of their broad-spectrum antimicrobial activity (Fuller *et al.* 2010) (Darouiche 1999) (Shirwaiker *et al.* 2011) (Shirwaiker *et al.* 2013) (Samberg *et al.* 2013) (Shirwaiker *et al.* 2014). In such systems, the positively charged silver electrodes release silver ions which attack bacteria cells in a multimodal fashion including penetrating the cell wall, denaturing enzymes, and disrupting DNA replication, which makes the development of bacterial resistance improbable. The effectiveness of such systems has been tested both *in vitro* and *in vivo* against a broad range of pathogens including antibiotic-resistant species such as methicillin-resistant *Staphylococcus aureus* (MRSA) (Wysk *et al.* 2010) (Nanda and Saravanan 2009) (Strohala *et al.* 2005) (Loh *et al.* 2009).

In order to develop the electrically-activated system for orthopaedic applications, Tan *et al.* investigated the effects of alternative cathode materials on the *in vitro* antimicrobial efficacy of the system (Tan *et al.* 2015). Based on a modified Kirby-Bauer diffusion test with a broad spectrum of pathogens, the results showed that the silver cathode in the LIDC-activated system could be substituted with other conductive metals without compromising on the system's antimicrobial efficacy. This study led to a strategy that minimized the quantity of silver in the system by partially substituting it with a biocompatible material such as titanium. Titanium is widely used in current orthopaedic implants due to its favorable mechanical properties and biocompatibility. *In vitro* and *in vivo* studies have previously shown surface treated titanium surfaces to promote osseointegration by stimulating bone formation at the cellular and molecular levels (Carlsson *et al.* 1986) (Le Guéhennec *et al.* 2007). Furthermore, titanium and its alloys possess good corrosion resistance and compressive yield strength which are critical to implants (Emsley 2001) (Tsvetkov 1995).

The effects of the design parameters on the antimicrobial efficacy of the LIDC-activated dual-metal (silver-titanium) implant system (DIS) were studied through a dynamic broth-based *in vitro* testing model, in which the system is immersed within a bacterial broth suspension and incubated in a shaker apparatus (Tan *et al.* 2014). The well-controlled homogenous environment and quantitative nature of this test model allows for more complex factorial experiments and provides an empirical foundation to build a mathematical model for the system. By adopting the broth-based testing model, anode surface area and current intensity were determined to be the two critical design parameters which influenced the antimicrobial efficacy of the system.

So far there has been limited research in developing an understanding and a quantitative model

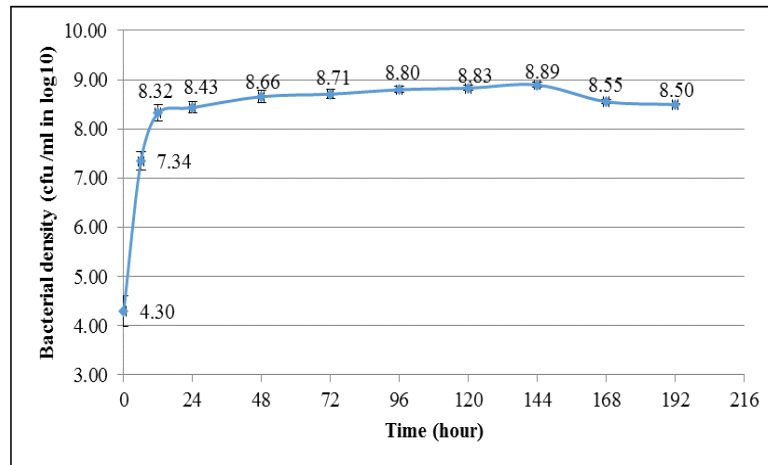


Fig. 1 Natural growth of *S. aureus* for 192 hour

of how the antimicrobial efficacy of the system changes in response to parameter variations. In order to establish a theoretical framework for analyzing the antimicrobial efficacy of the DIS in a nutrient-rich fluid environment, a differential model is derived in this study based on the classical *in vitro* Pharmacokinetic/Pharmacodynamic (PK/PD) modeling approach. The PK/PD model integrates pharmacokinetic and pharmacodynamic components into one set of mathematical expressions that allows the description of the time course of effect intensity in response to administration of a drug dose (Derendorf and Meibohm 1999). Models of antimicrobials have to include at least a sub-model of microorganism replication and a sub-model of antimicrobial drug effects (Vaddady *et al.* 2010). In this study, a symbolic regression model was developed to describe the antimicrobial effect of the DIS and to establish the relationships between the critical design parameters and the antimicrobial efficacy of the system.

## 2. Antimicrobial efficacy test

### 2.1 Bacterial strains and media

A *S. aureus* strain (ATCC 25213) was used in this study. The bacteria was cultured on Mueller Hinton agar (BD Diagnostics, Sparks, MD) and stored at 4°C. For each experiment, a colony from the refrigerated agar plate was inoculated in 2 ml Mueller Hinton broth (BD Diagnostics) and incubated at 37°C overnight. The bacterial concentration of the broth were estimated through optical density measurements (OD 600 spectrophotometer, Shimadzu Inc, Norcross, GA;  $\lambda=600$  nm). The broth was serially diluted to  $10^4$  colony forming units (cfu)/ml for each experiment.

In order to characterize the natural growth of the *S. aureus*, four samples of 15 ml bacterial-inoculated Mueller Hinton broth were prepared with the initial concentration of  $10^3$ – $10^4$  cfu/ml and incubated at 37°C. The bacterial concentration was estimated at 10 time points over a 192 hour (eight days) interval. A logarithmic plot of natural growth of *S. aureus* in the broth over eight days is presented in Fig. 1.

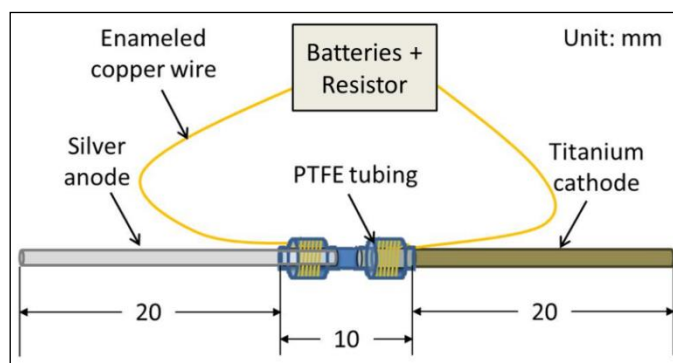


Fig. 2 A schematic of the LIDC-activated silver-titanium implant system

## 2.2 Fabrication of the electrically activated implant prototype

The implant prototype (Fig. 2) consisted of a silver anode and a titanium cathode ( $\emptyset$  1 mm, Advent Research Materials, Oxford, UK), which were connected to an electric circuit by enameled copper wires ( $\emptyset$  0.2 mm Radioshack, Fort Worth, TX). The electrodes were assembled into a heat shrunk Polytetrafluoroethylene (PTFE) tubing separator (Zeus Inc., Orangeburg, SC) which held two electrodes in alignment and sealed the joints to obtain the necessary silver-polymer-titanium implant configuration. This configuration mimics an orthopaedic implant like an intramedullary rod or hip stem. Four 1.5 V AA batteries (RadioShack®, Cary, NC) were connected in series serving as the power source to provide a current of 1–14  $\mu$ A with corresponding resistors. The system is in a passive state (no system current) due to the insulating divider between electrodes unless it is surrounded by electrically conductive fluid media. In the latter case, the fluids complete the electric circuit between the electrodes resulting in the active release of  $\text{Ag}^+$  from the silver anode.

The implant prototype was submerged in 10 ml bacteria-inoculated broth in a 15 ml centrifuge tube and energized by low intensity direct current for 48 hours. The entire experimental setup was

Table 1 Experimental design parameters of the antimicrobial efficacy test

Design Parameters	Levels
Electrode separation distance (mm)	10
	20
Anode surface area ( $\text{mm}^2$ )	31.4
	62.8
	94.2
Current frequency (Hz)	0
	1
Current intensity ( $\mu$ A)	1
	7
	14

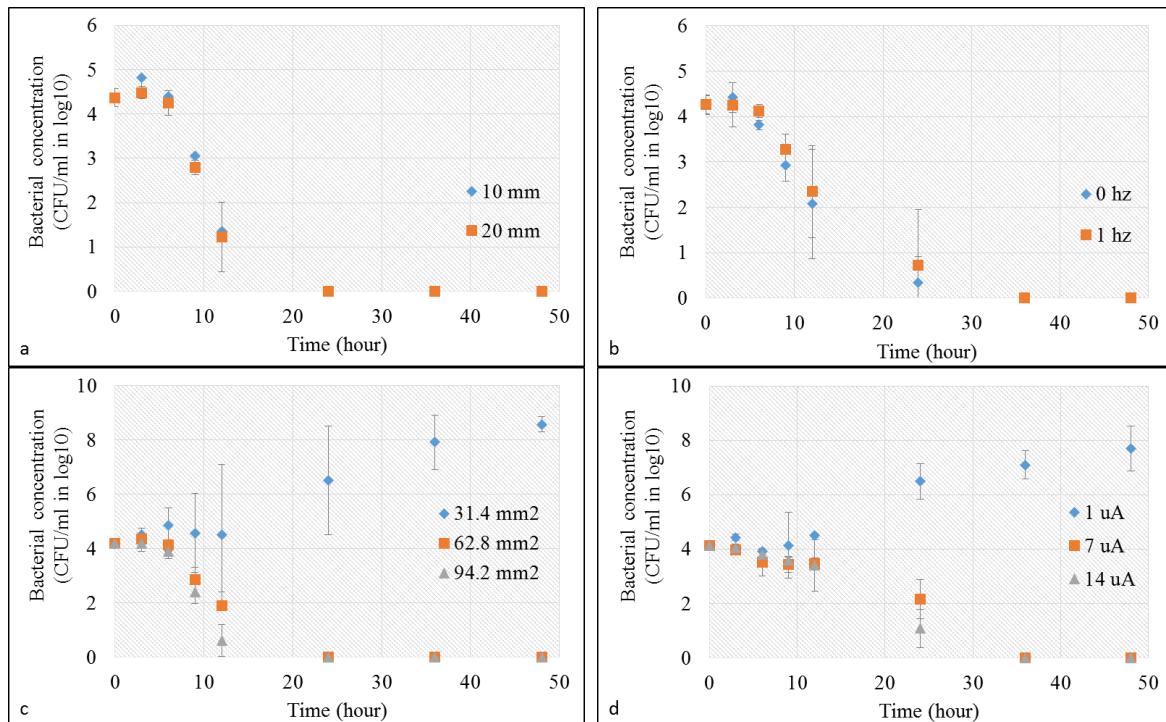


Fig. 3 Empirical time-kill curves for DIS with different (a) electrode separation distance, (b) current frequency, (c) current intensity, and (d) anode surface area

incubated in an incu-shaker at 37°C with shaking speed of 100 rpm to have homogenized bacteria distribution in the broth. The bacterial concentration was measured periodically at 0, 3, 6, 9, 12, 24, 36 and 48 hour time periods using the standard plate counting method. Four design parameters of the silver-titanium implant system including electrode separation distance, anode surface area, current intensity and current frequency were investigated using four independent one-way factorial experiments ( $n=12$  per factorial level). The experimental design is given in Table 1.

The empirical time-kill curves are presented in Fig. 3. They demonstrate that the DIS reduces the bacterial concentration after 12 hours. All test groups completely kill bacteria after 36 hours except for the group with current intensity of 1  $\mu\text{A}$  and the group with anode surface area of 31.4  $\text{mm}^2$ . For these two groups, the bacterial concentration decreases in the first 12 hours but rises subsequently, indicating a decline in the DIS antimicrobial efficacy over time.

### 3. Model development

#### 3.1 Model structure

The modeling of the relationship between design parameters and antimicrobial efficacy of the system is based on the empirical time-kill curves discussed in the previous section. Fig. 4 gives an overview of the different activities and interactions that occur when the implant system is active. In modeling the system behavior, there are two basic components: 1) silver-susceptible,

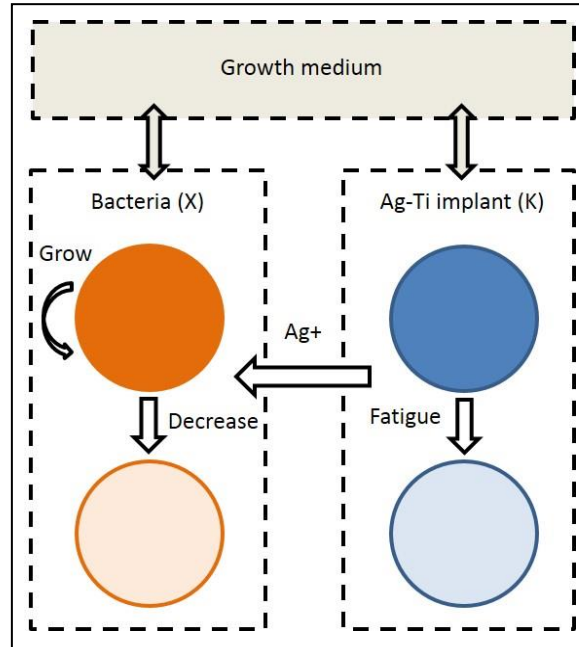


Fig. 4 Illustration of the antimicrobial process based on the modified PK/PD model

growing bacteria with first-order growth rate constant ( $r_0$ ), and 2) the bactericidal effect of released silver ions with a variable rate  $k$ . For the first component, according to population growth model, the bacterial growth rate is proportional to both the existing population and the amount of available resources. Eqs. (1) and (2) describe the function of the bacterial concentration in the broth in presence of the implant system

$$\begin{cases} \frac{dx}{dt} = r_0 \times D(x) - k \times D(x) \\ x(0) = x_0 \end{cases} \quad (1)$$

$x$ =bacterial concentration at time  $t$

$r_0$ =initial growth rate of bacterial cells

$D(x)$ =degree of the saturation concentration

$$D(x) = x \left( 1 - \frac{x}{x_{max}} \right) \quad (2)$$

$x_{max}$ =the maximum achievable bacterial concentration in the broth.

### 3.2 Natural growth of *S. aureus*

In an ideal environment without any interference factors, the bacterial growth can be modeled with four different phases: lag phase, exponential phase, stationary phase, and decline phase (Baranyi and Roberts 1994). According to the experimentally determined growth curve for *S. aureus*, (Fig. 1), the lag phase is indiscernible and therefore can be excluded in the model. The exponential phase lasts for 12 hours followed by the stationary phase. No sharp decrease or

dramatic change is detected afterwards. Because the duration of the kill-curve experiments was 48 hours, it is appropriate to not consider the decline phase in the first component of the model.

Based on a regression analysis of Fig. 1,  $r_0$  in Eq. (1) and  $x_m$  in Eq. (2) are estimated to be 1.3525 and  $10^{8.9}$  respectively. Based on these two constants, the following basic assumptions are made in developing the modified PK/PD model:

1) All batches of bacteria have an initial concentration of  $10^4$  cfu/ml, which was the experimental setting, and the initial natural growth rate  $r_0=1.3525$ .

2) All batches of bacteria reach the same maximal concentration of  $10^{8.9}$  cfu / ml.

3) After the bacterial concentration decreases to zero in a logarithmic manner which indicates that the majority of bacteria have been killed, it stays at zero.

### 3.3 Kinetic analysis of antimicrobial activity

To fit the empirical time-kill curves, we establish a symbolic regression model for the intensity of the antimicrobial efficacy exerted by the system, which is described as first order derivative of the bacterial concentration. The antimicrobial efficacy of the system  $k$  at time  $t$  is given as Eq. (3)

$$\begin{aligned} k(0) &= k_0 \\ k(t) &= k_0(1 - \delta)^t t \\ 0 &< \delta < 1 \end{aligned} \quad (3)$$

$\delta$ =accumulated fatigue rate of the antimicrobial efficacy.

The changing rate of bacterial concentration is given by

$$r(t) = r_0 - k(t) = r_0 - k_0(1 - \delta)^t t \quad (4)$$

Eq. (1) can therefore be modified and represented as Eq. (5)

$$\begin{aligned} \frac{dx}{dt} &= x \left(1 - \frac{x}{x_m}\right) [r_0 - k_0(1 - \delta)^t t] \\ x(0) &= x_0 \end{aligned} \quad (5)$$

Eq. (5) can be solved by the method of separation of variables

$$\int \frac{1}{x \left(1 - \frac{x}{x_m}\right)} dx = \ln\left(\frac{x}{x_m - x}\right) = \int r(t) dt \quad (6)$$

Given that  $x(0) = x_0$ ,

$$x(t) = \frac{x_m}{1 + \left(\frac{x_m}{x_0} - 1\right) e^{-\int_0^t r(s) ds}} \quad (7)$$

The integration of  $r(t)$  from 0 to time  $t$  is given by

$$\begin{aligned}\int_0^t r(x)dx &= \int_0^t (r_0 - k_0(1-\delta)^x x)dx = \int_0^t r_0 dx - k_0 \int_0^t (1-\delta)^x x dx \\ &= r_0 t - \frac{k_0}{\ln(1-\delta)} \left[ t(1-\delta)^t - \frac{(1-\delta)^t - 1}{\ln(1-\delta)} \right]\end{aligned}\quad (8)$$

Substituting Eq. (8) into Eq. (7) results in Eq. (9)

$$x(t) = \frac{x_m}{\left\{ 1 + \left( \frac{x_m}{x_0} - 1 \right) \exp \left[ r_0 t - \frac{k_0}{\ln(1-\delta)} \left[ t(1-\delta)^t - \frac{(1-\delta)^t - 1}{\ln(1-\delta)} \right] \right] \right\}}\quad (9)$$

The logarithm of Eq. (9) results in Eq. (10)

$$L(t) = L_m - \text{Log}_{10} \left\{ 1 + \left( \frac{x_m}{x_0} - 1 \right) \exp \left[ -r_0 t + \frac{k_0}{\ln(1-\delta)} \left[ t(1-\delta)^t - \frac{(1-\delta)^t - 1}{\ln(1-\delta)} \right] \right] \right\}\quad (10)$$

For an arithmetic progression  $T_N = (t_1, t_2, \dots, t_{N-1}, t_N)$ , the bacterial concentration at time  $t_n$  is given by

$$D(t_n) = \begin{cases} \max\{0, L(t_n)\}, & D(t_{n-1}) > 0 \\ 0, & D(t_{n-1}) = 0 \end{cases}\quad (11)$$

For  $t_n \in T_N$

### 3.4 Model parameters

With a fixed initial bacterial concentration  $x_0$ , the simulated concentration plot was determined using  $k_0$  and  $\delta$ , which are henceforth referred to as the antimicrobial efficacy parameters (AEP). For each factorial level in the empirical time-kill curves, the AEP values that resulted in the maximal  $R^2$  (optimal AEP) were assigned to fit the empirical data. The maximal  $R^2$  was searched using the enumeration method, which entails calculating the  $R^2$  of plots with all combinations of AEP in a finite set of reasonable values. Because there were eight time points in the experiment, only the corresponding eight simulated data points were used in calculating the  $R^2$ . The maximal antimicrobial capacity (MAC) for a given set of AEP, defined as the maximal level of initial bacterial concentration in the 10 ml MH broth in which the DIS could kill all bacteria (*S. aureus* in this study), was estimated by the maximal  $x_0$  with which the simulated time-kill curve reached zero at the 48 hour interval. Similarly, the MAC was calculated by enumerating a finite set of  $x_0$ . The analysis was performed in MS Excel 2013® with MS Visual Basic for Application 7.0. The algorithms (pseudo codes) used to determine the optimal AEP and MAC are presented in Fig. 5. For each replicate of the experiment, a set of AEP values were determined with the corresponding  $R^2$  indicating the goodness-of-fit of the model. The mean AEP values from the three replicates were used in the final differential model.

Fig. 6 shows the simulated time-kill curves generated by the antimicrobial efficacy model given in Eq. 11 with different AEPs (by MS EXCEL® 2013). It should be also noted that with fixed AEPs, different initial bacterial concentrations ( $x_0$ ) resulted in variations in the time-kill curves (Fig. 6(b)). For example, the MAC for the setting of  $k_0=0.7$  and  $\delta=0.1$  was between  $10^5$  and  $10^6$

cfu/ml.

## 4. Results and discussion

### 4.1 Simulated time-kill curves

The simulated time-kill curves for the antimicrobial efficacy test are presented in Fig. 7. The estimated AEPs and the MACs for all parameters are summarized in Table 2. It can be observed that the differential model (Eq. (11)) demonstrated excellent reliability with high level of goodness-of-fit; the  $R^2$  values were greater than 70% for all groups. A 100% change of electrode separation distance only caused a 7.6% increase in the initial antimicrobial efficacy ( $k_0$ ) and an 8.9% increase in the accumulated fatigue rate ( $\delta$ ). This translated into a variation in MAC from  $10^{4.77}$  cfu/ml to  $10^{4.67}$  cfu/ml. For current frequency, a change from 0 hz to 1 hz only caused a 5.7% decrease in  $k_0$  and a 3.9% decrease in  $\delta$  corresponding to a change in MAC from  $10^{4.85}$  cfu/ml to  $10^{4.56}$  cfu/ml. An increase in anode surface area from  $31.4 \text{ mm}^2$  to  $62.8 \text{ mm}^2$  resulted in an 11% decrease in  $k_0$  and a 42.5% decrease in  $\delta$ . A MAC = 0 for  $31.4 \text{ mm}^2$  implies that the device with

```

Step 1. Determine the optimal AEP:
Datapoint(1-8) = the empirical data points
D(1-8) = the simulated data points calculated according to the differential model
meanData = mean(Datapoint(1),Datapoint(2),..., Datapoint (8))
Rtt =  $\sum_{i=1}^8 (\text{Datapoint}(i) - \text{meanData})^2$ 
For k = 0.3 to 1.3
  For delta = 0.01 to 0.3
    Rer =  $\sum_{i=1}^8 (\text{Datapoint}(i) - D(i))^2$ 
    If Rer < min_Rer Then
      min_Rer = Rer
      k_op = k
      delta_op = delta
    End if
    delta = delta + 0.001
  Loop
  k = k + 0.01
Loop
R_square = 1 - min_Rer/Rtt

Step 2. Determine the MAC
For x0 = 2 to 8.89
  Bacterial density (0) = x0
  For t = 1 to 48
    Calculate D(t) with k_op and delta_op
  If D(48) = 0 Then
    max_x1 = x1
  End If
  x1 = x1 + 0.01
Loop

```

Fig. 5 Algorithms for determining (a) the optimal AEP and (b) the MAC

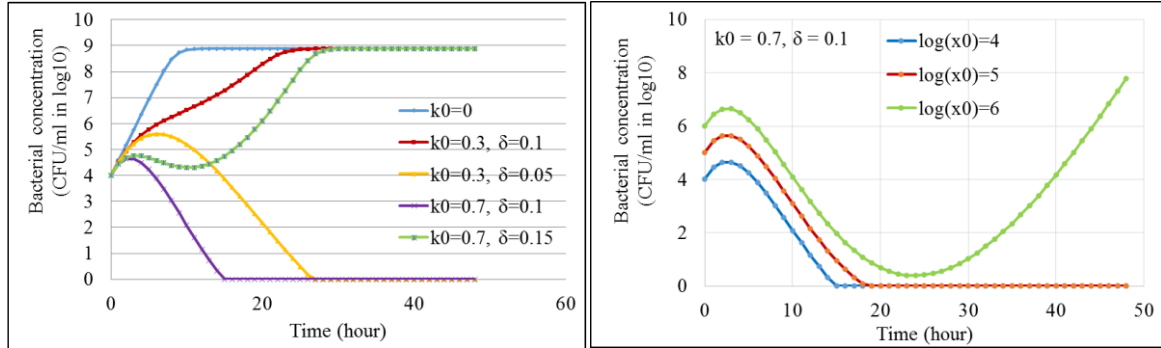


Fig. 6 Plots of the differential models (a) with same  $x_0$  but different  $k_0$  and  $\delta$ , and (b) with same  $k_0$  and  $\delta$  but different  $x_0$

Table 2 AEP and MAC for tested parameters

Parameters	Levels	$k_0$	Diff	$\delta$	Diff	MAC	$R^2$
Electrode separation distance	10 mm	0.66		0.089		$10^{4.77}$ cfu / ml	0.997
	20 mm	0.71	7.6 %	0.097	8.9 %	$10^{4.67}$ cfu / ml	0.988
Anode surface area	31.4 mm <sup>2</sup>	0.8		0.179	2.8 - 42.5 %	0 cfu / ml	0.973
	62.8 mm <sup>2</sup>	0.71	8.5 - 11.3 %	0.106		$10^{4.42}$ cfu / ml	0.989
	94.2 mm <sup>2</sup>	0.77		0.103		$10^{6.52}$ cfu / ml	0.987
Current intensity	1 $\mu$ A	0.2		0.05		0 cfu / ml	0.869
	7 $\mu$ A	0.63	1.6 - 215 %	0.1	0 - 100 %	$10^{4.06}$ cfu / ml	0.700
	14 $\mu$ A	0.62		0.1		$10^{4.47}$ cfu / ml	0.892
Current frequency	0 hz	0.7		0.103		$10^{4.85}$ cfu / ml	0.937
	1 hz	0.66	5.7 %	0.099	3.9 %	$10^{4.56}$ cfu / ml	0.823

anode surface area of 31.4 mm<sup>2</sup> is not capable of reducing the bacterial concentration. An increase in anode surface area from 62.8 mm<sup>2</sup> to 94.2 mm<sup>2</sup> resulted in an 8.5 % increase in  $k_0$  and a 2.8% decrease in  $\delta$ , which translated to an increase in MAC from  $10^{4.42}$  cfu/ml to  $10^{6.52}$  cfu/ml. Finally, for current intensity, a change from 1  $\mu$ A to 7  $\mu$ A resulted in a 215% increase in  $k_0$  and a 100% increase in  $\delta$ . The MAC for the current intensity of 1  $\mu$ A was zero. However, increasing the intensity from 7  $\mu$ A to 14  $\mu$ A, only caused a 1.6% increase in  $k_0$  and no change in  $\delta$ , which translated to an increase in MAC from  $10^{4.06}$  cfu/ml to  $10^{4.47}$  cfu/ml.

As the results in Table 2 demonstrate, current intensity and anode surface area had non-linear effects on the bactericidal rate and the fatigue rate of the DIS. The relationships between the AEPs and these two design parameters can be described as logarithmic regression models as Eq. (12) and (13)

$$k = 0.134 \ln(C) + 0.336 \quad (12)$$

$$\delta = 0.009 \ln(C) - 0.073 \ln(A) + 0.5 \quad (13)$$

$C$ =current intensity ( $\mu$ A)

$A$ =anode surface area ( $\text{mm}^2$ )

#### 4.2 Mechanisms of system fatigue

The modified PK/PD model demonstrates that the current intensity and the anode surface area influence the antimicrobial efficacy in two aspects. Anode surface area has a negligible impact on the initial antimicrobial efficacy but has a significant non-linear negative influence on the accumulated fatigue rate, which is directly related to the effective duration of the system. Current intensity has a non-linear positive impact on both initial antimicrobial efficacy and the accumulated fatigue rate. The reason for this phenomenon can be explained by the following considerations and observations.

Since the total electric quantity ( $Q_E$ ) transferred between electrodes is constant, the variation of anode surface area essentially changes the ratio of current to the anode surface over which that current is applied, namely surface current density (SCD) ( $\mu\text{A}/\text{mm}^2$ ), which reflect the electrochemical reaction rate of the silver anode in the energized status

$$SCD = \frac{Q_E/t}{S} = \frac{I}{S} \quad (14)$$

$t$ =energizing time (s)

$S$ =anode surface area ( $\text{mm}^2$ )

$I$ =current intensity ( $\mu\text{A}$ )

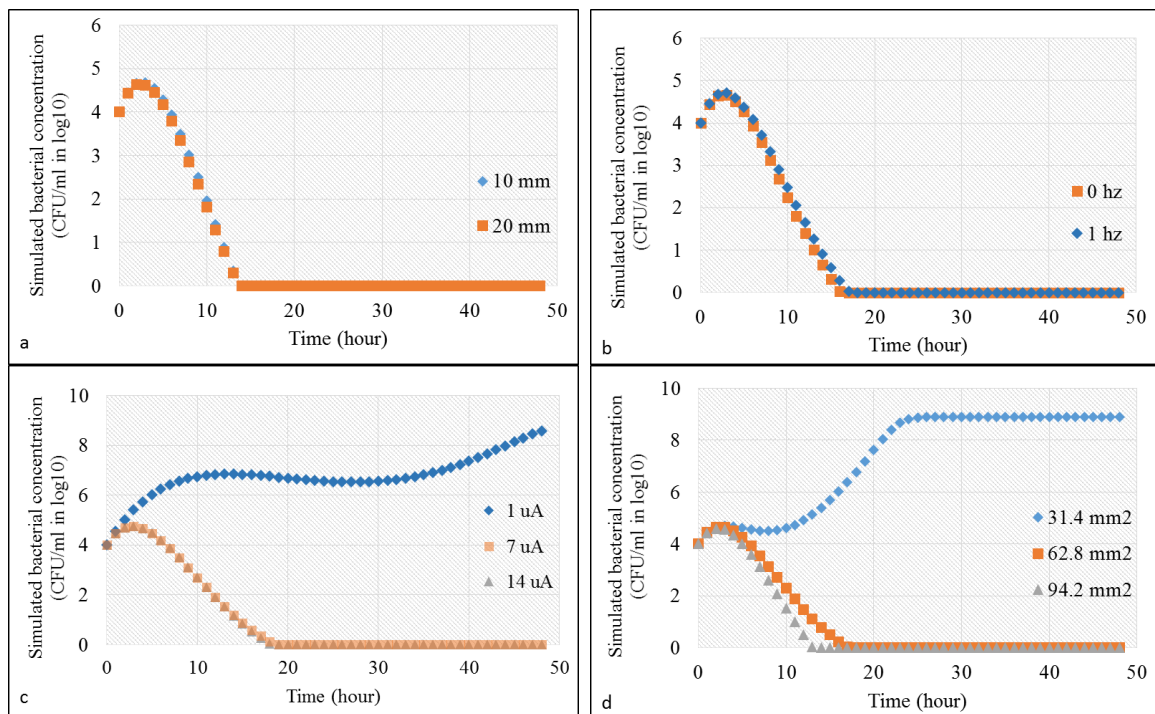


Fig. 7 Simulated time-kill curves for DIS with different (a) electrode separation distance, (b) current frequency, (c) current intensity, and (d) anode surface area test

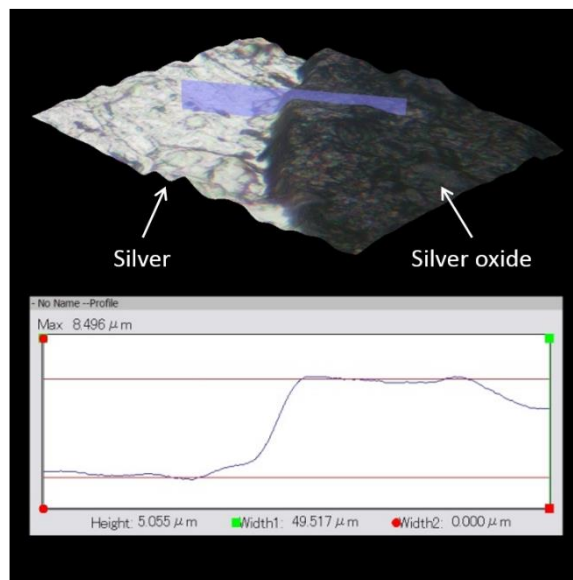


Fig. 8 A silver oxide layer sample observed by Hirox® KH-7700 digital microscope with magnification of 3500

It was observed in the experiments that higher SCD resulting from smaller anode area would lead to faster surface oxidization rate. In the experiments, the silver anodes of  $31.4 \text{ mm}^2$  became completely oxidized after 12 hour while the anodes of the other two groups were only partially oxidized. The surface was covered by a thin layer of black silver oxide, which is the product of the reaction between silver and nutrients such as proteins in the broth medium. The oxidized silver anodes were examined under a Hirox® KH-7700 digital microscope system (Hirox-USA, Hackensack, NJ). The silver oxide formed a cliff-shape raised platform at the boundary between the area exposed to broth media and the hidden area protected by PTEF tubing. The thickness of this silver oxide layer was found to be within  $2.9 - 5.2 \mu\text{m}$ . A sample digital image of the silver oxide layer is presented in Fig. 8.

The silver oxide coating created considerably high resistance which inhibited efficient oligodynamic iontophoresis. In other words, the system became less effective. Given that the kinetic  $\text{Ag}^+$  in the growth media would easily potentially bind with other negative charges and lose the antimicrobial potency, the accumulative effect of the antimicrobial efficacy of the system was limited. Therefore the group with a smaller anode surface area only inhibited the bacterial growth for a certain initial period but the bacterial concentration rose again as the device compromised on its antimicrobial capability over time. On the other hand, groups with the larger anode surface area had a lower SCD resulting in lower accumulative fatigue rate, which implied longer effective period of antimicrobial potency. The results demonstrate that an increase in anode surface area from  $62.8 \text{ mm}^2$  to  $94.2 \text{ mm}^2$  increases the bactericidal capacity by nearly two orders of magnitude.

#### 4.3 Applications of the model

Several prior studies have adopted the modified Kirby-Bauer method to investigate the

parameter effects of silver systems on their antimicrobial efficacy which is correlated to the size of the inhibition zones on the surface of the bacteria-inoculated agar medium after a given interval (typically between 12 - 24 h). This semi-quantitative testing method is a good indicator of the system's efficacy. However, it does not provide an effective way to understand and model in a quantifiable manner how the system impacts the bacterial growth over time and how the intensity of the antimicrobial efficacy changes according to parameter variations. In addition, the agar-based testing method cannot provide accurate information for test intervals longer than 24 hours because it is difficult to differentiate between surviving and dead cells after the bacteria colonies have formed.

This study characterized the time course of events observed in a bacterial system when exposed to electrically-activated silver ions. The modified PK/PD model developed in this study quantifies the relationships between the antimicrobial efficacy and two critical system parameters. According to the regression models given in Eq. (12) and Eq. (13), for a given anode surface area, there will be a threshold of current intensity which maintains minimal SCD to guarantee the bactericidal effect. For example, an implant device with an anode surface area of 62.8 mm<sup>2</sup> requires at least 6  $\mu$ A current to reduce the bacterial concentration in the broth medium with a starting concentration of 10<sup>4</sup> cfu/ml. It is also possible to reduce the fatigue rate of antimicrobial efficacy by increasing the anode surface because, because the SCD is proportional to the anode surface area at a given current intensity level.

The PK/PD relationship for antimicrobials has been studied for decades (Craig 1995.) (Gustafsson *et al.* 2001) (Liu *et al.* 2005) (Nielsen *et al.* 2006) (Wang *et al.* 2015) due to its ability to simulate different concentration-time profiles which offer important information complementary to *in vivo* studies (Marshall *et al.* 2006) (Czock and Keller 2007). The semi-mechanistic model of the silver-titanium implant system was derived from a common PK/PD model premised on cell growth and killing processes. It includes a sub-model of microorganism replication and a sub-model of antimicrobial drug effects. The silver-induced antimicrobial activity in this study showed an initial phase with a mild inhibition, followed by a rapid killing, the rate of which declined over time. The exact mechanisms underlying this phenomenon still remain to be investigated. Some related studies suggested that silver ions attack bacterial cells in multiple modes, including penetrating the cell wall, denaturing enzymes of the target cell by binding to reactive groups and inactivating DNA molecules (Feng *et al.* 2000). Increased knowledge regarding the interactions of silver ions with medium could aid in the further development of a more mechanistic PK/PD model to describe the biological system.

In summary, the mathematical model provides further insight into the effects of electrically-activated silver ions. It enables simulations of the implant system with different design parameters and therefore allows prediction of antimicrobial effects in nutrient-rich fluid environments. After further refinement, the model could serve as a tool for the development of optimal designs or even to derive potential clinical treatment strategies.

## 5. Conclusions

A modified PK/PD model was developed for the *in vitro* antimicrobial effects of the electrically-activated silver-titanium implant system against an *S. aureus* strain. The model demonstrated the influence of current intensity and anode surface area on the initial antimicrobial efficacy and fatigue rate of the system in an interactive manner. The effective ranges of these two

parameters can be estimated for the system to maintain significant antimicrobial efficacy. The model may be applied to other strains and can provide a tool for the development of antimicrobial implantable medical products.

## Acknowledgments

The research described in this paper was supported by a grant from NC State's 2013 Research and Innovation and Seed Funding (RISF) program. The authors thank Ms. Patty Spears and Ms. Mitsu Suyemoto from NC State University's College of Veterinary Medicine for their valuable and constructive suggestions during the antimicrobial efficacy testing experiments.

## References

- Anima, Nanda and Saravanan, M. (2009), "Biosynthesis of silver nanoparticles from *Staphylococcus aureus* and its antimicrobial activity against MRSA and MRSE", *Nanomed. Nanotech. Biol. Med.*, **5**(4), 452-456.
- Baranyi, J. and Roberts, T.A. (1994), "A dynamic approach to predicting bacterial growth in food", *Int. J. Food Microbiol.*, **23**(3), 277-294.
- Berberi, E., Hanssen, A., Duffy, M., Steckelberg, J., Ilstrup, D., Harmsen, W. and Osmon, D. (1998), "Risk factors for prosthetic joint infection: case-control study", *Clin. Infect. Dis.*, **27**(5), 1247-1254.
- Carlsson, L., Röstlund, T., Albrektsson, B., Albrektsson, T. and Brånemark, P. (1986), "Osseointegration of titanium implants", *Acta Orthop. Scand.*, **57**(4), 285-289.
- Craig, W.A. (1995), "Interrelationship between pharmacokinetics and pharmacodynamics in determining dosage regimens for broad-spectrum cephalosporins", *Diagn. Microbiol. Infect. Dis.*, **22**(1), 89-96.
- Czock, D. and Keller, F. (2007), "Mechanism-based pharmacokinetic-pharmacodynamic modeling of antimicrobial drug effects", *J. Pharmacokinet. Pharmacodyn.*, **34**(6), 727-751.
- Darouiche, R.O. (1999), "Anti-infective efficacy of silver-coated medical prostheses", *Clin. Infect. Dis.*, **29**(6), 1371-1377.
- Derendorf, H. and Meibohm, B. (1999), "Modeling of pharmacokinetic/pharmacodynamic (PK/PD) relationships: Concepts and perspectives", *Pharm. Res.*, **16**(2), 176-185.
- Emsley, J. (2001). *Nature's Building Blocks: An A-Z Guide to the Elements*, Oxford, Oxford University Press.
- Feng, Q.L., Wu, J., Chen, G.Q., Cui, F.Z., Kim, T.N. and Kim, J.O. (2000), "A mechanistic study of the antibacterial effect of silver ions on *Escherichia coli* and *Staphylococcus aureus*", *J. Biomed. Mater. Res. A*, **52**(4), 662-668.
- Fuller, T.A., Wysk, R.A., Charumani, C., Kennett, M., Sebastienelli, W.J., Abrahams, R., Shirwaiker, R.A., Voigt, R.C. and Royer, P. (2010), "Developing an engineered antimicrobial/prophylactic system using electrically activated bactericidal metals", *J. Mater. Sci. Mater. Med.*, **21**(7), 2103-2114.
- Gustafsson, I., Lowdin, E., Odenholt, I. and Cars, O. (2001), "Pharmacokinetic and pharmacodynamic parameters for antimicrobial effects of cefotaxime and amoxicillin in an in vitro kinetic model", *Antimicrob. Agents Chemother.*, **45**(9), 2436-2440.
- Harris Williams & Co. (2011), *Orthopedic Implants-A Global Market Overview*, Hyderabad, India, Industry Experts.
- Le Guéhennec, L., Soueidan, A., Layrolle, P. and Amouriq, Y. (2007), "Surface treatments of titanium dental implants for rapid osseointegration", *Dent. Mater.*, **23**(7), 844-854.
- Liu, P., Rand, K.H., Obermann, B. and Derendorf, H. (2005), "Pharmacokinetic-pharmacodynamic modelling of antibacterial activity of cefpodoxime and cefixime in in vitro kinetic models", *Int. J. Antimicrob. Agents*, **25**(2), 120-129.

- Loh, J.V., Percival, S.L., Woods, E.J., Williams, N.J. and Cochrane, C.A. (2009), "Silver resistance in MRSA isolated from wound and nasal sources in humans and animals", *Int. Wound J.*, **6**(1), 32-38.
- Marshall, S., Macintyre, F., James, I., Krams, M. and Jonsson, N.E. (2006), "Role of mechanistically-based pharmacokinetic/pharmacodynamic models in drug development: a case study of a therapeutic protein", *Clin. Pharmacokinet.*, **45**(2), 177-197.
- Nielsen, E.I., Viberg, A., Löwdin, E., Cars, O., Karlsson, M.O. and Sandström, M. (2006), "Semimechanistic Pharmacokinetic/Pharmacodynamic model for assessment of activity of antibacterial agent from time-kill curve experiments", *Antimicrob. Agents Chemother.*, **51**(1), 128.
- Samberg, M.E., Tan, Z., Monteiro-Riviere, N.A., Orndorff, P.E. and Shirwaiker, R.A. (2013), "Biocompatibility analysis of an electrically-activated silver-based antibacterial surface system for medical device applications", *J. Mater. Sci. Mater. Med.*, **24**(3), 755-760.
- Shirwaiker, R.A., Samberg, M.E., Cohen, P.H., Wysk, R.A. and Monteiro-Riviere, N.A. (2013), "Nanomaterials and synergistic low-intensity direct current (LIDC) stimulation technology for orthopedic implantable medical devices", *WIREs Nanomed. Nanobiotechnol.*, **5**(3), 191-204.
- Shirwaiker, R.A., Wysk, R.A., Kariyawasam, S., Carrion, H. and Voigt, R.C. (2011), "Micro-scale fabrication and characterization of a silver-polymer-based electrically activated antibacterial surface", *Biofabrication*, **3**(1), 015003.
- Shirwaiker, R.A., Wysk, R.A., Kariyawasam, S., Voigt, R.C., Carrion, H. and Nembhard, H. (2014), "Interdigitated silver-polymer-based antibacterial surface system activated by oligodynamic iontophoresis - An empirical characterization study", *Biomed. Microdevices*, **16**(1), 1-10.
- Strohala, R., Schellingb, M., Takacs, M., Jurek, W., Gruber, U. and Offner, F. (2005), "Nanocrystalline silver dressings as an efficient anti-MRSA barrier: a new solution to an increasing problem", *J. Hosp. Infect.*, **60**(3), 226-230.
- Tan, Z., Ganapathy, A., Orndorff, P.E. and Shirwaiker, R.A. (2015), "Effects of cathode design parameters on in vitro antimicrobial efficacy of electrically-activated silver-based iontophoretic system", *J. Mater. Sci. Mater. Med.*, **26**(1), 1-10.
- Tan, Z., Xu, G. and Shirwaiker, R.A. (2014), "In vitro quantitative analysis on the antimicrobial performance of the dual-metal implant system", *IIE Annual Conference and Expo*, Montreal.
- Tsvetkov, V.V. (1995), "Corrosion-resistant titanium alloys", *Pharm. Chem. J.*, **29**(8), 564-566.
- Vaddady, P.K., Lee, R.E. and Meibohm, B. (2010), "In vitro pharmacokinetic/pharmacodynamic models in anti-infective drug development: focus on TB", *Future Med. Chem.*, **2**(8), 1355-1369.
- Virk, A. and Osmon, D. (2001), "Prosthetic joint infection", *Curr. Treat. Option. Infect. Dis.*, **351**(16), 287-300.
- Wang, Z., Butner, J.D., Cristini, V. and Deisboeck, T.S. (2015), "Integrated PK-PD and agent-based modeling in oncology", *J. Pharmacokinet. Pharmacodyn.*, doi:10.1007/s10928-015-9403-7.
- Wiedel, J. (2002), "Salvage of infected total knee fusion: the last option", *Clin. Orthop. Relat. Res.*, **404**, 139-142.
- Wysk, R.A., Sebastianelli, W.J., Shirwaiker, R.A., Bailey, G.M., Charumani, C., Kennett, M., Kaucher, A., Abrahams, R., Fuller, T.A., Royer, P., Voigt, R.C. and Cohen, P.H. (2010), "Prophylactic bactericidal orthopedic implants - animal testing study", *J. Biomed. Sci. Eng.*, **3**(9), 917-926.